

Assessment of Soil Erosion Susceptibility, Spatial Sediment Delivery Processes and Control Strategies at the Nzoia River Catchment in Kenya

¹Kipyegon Koskei., ²Cherono Janeth

¹Department of Alternative Energy, Rural Electrification and Renewable Energy Corporation,
Nairobi, Kenya

²Agricultural Extension Consultant, South Rift Litein, Kenya

DOI: <https://doi.org/10.51244/IJRSI.2024.11100015>

Received: 23 September 2024; Accepted: 03 October 2024; Published: 04 November 2024

ABSTRACT

The Nzoia basin is among the most densely populated regions in Western Kenya, with an average density of up to 450 people per square kilometre. Cereal farming accounts for over half of the land usage in the basin. The massive conversion of land from forest to cropland and grassland in the region has significantly impacted soil erosion and reduced soil fertility. Several studies have been undertaken in the catchment, principally on potential soil loss; however, no extensive research has been conducted on the spatial sediment delivery processes or on establishing the best land management practices for the catchment. This study simulates the basin's susceptibility to erosion using the RUSLE model, examines the spatial sediment delivery process, and undertakes scenario analysis to establish the best erosion control practices for the catchment. The RUSLE factors were combined in ILWIS GIS to create functions for soil erosion and sediment transport capacity, which were applied to compute the potential annual soil loss for each pixel. The formulated sediment routing algorithm directed the sediments toward the river and the lake. The results from the study show that potential annual soil loss varied from 0.00 in the lowlands to 4,577 tonnes/ha/year in the highland areas, with the catchment's total potential soil loss estimated at 8,380,000 tonnes/year. The basin's sediment yield at Lake Victoria was 2,494,575 tons/year, translating to a sediment delivery ratio of about 29%. The cropland regions were the dominant contributors of eroded sediments. The scenario analysis applied practical agronomic and mechanical erosion control methods to croplands, demonstrating that adopting multiple soil erosion control strategies could effectively reduce soil loss across the catchment. Areas with high erosion are primarily found in the sloping regions of the catchment, especially around Mt. Elgon, Chereng'anyi Hills, Kipkaren, and Kapsokwony. The spatial soil erosion and deposition hazard maps generated in this study should be used as practical guides for combating land degradation in the Nzoia River catchment.

Keywords: Land Degradation, RUSLE, Sediment Delivery Processes, Erosion Control Methods, Sediment Yield, Scenario Analysis, ILWIS

INTRODUCTION

Nzoia basin is among the regions in Western Kenya that support the densest populations, with average densities of up to 450 persons per square kilometre [1]. This basin covers approximately 12,900 km² and is characterised by diverse topography, ranging from the highlands of Mount Elgon (4,321 m above sea level) to the lowlands near Lake Victoria (1,134 m above sea level) in the southwest. This diverse landscape, intense rainfall patterns, and human activities contribute to the region's complex soil erosion dynamics [2]. Agricultural activities account for about half of the land usage in the basin [3].

Wind and water erosion usually occur in most parts of the country, but the most conspicuous process in the basin is erosion by water. It happens over the entire basin and peaks during the wet season, mainly in April to May and August to September, and highly turbid river flows can attest to this during these periods. A

study by [4] in the Lake Victoria basin, of which the Nzoia basin is part, established that areas dominated by crops and grasses were approximately 16 times more likely to be affected by severe sheet, rill, or gully erosion than areas dominated by trees. Also, from the same study, they established that the sediment delivery ratio varies spatially from one catchment to the next, with the Nyando River consistently having the highest levels of turbidity, the Nzoia and Yala Rivers registering similar intermediate levels, and the Sondu-Miriu River having the lowest levels. A study by [28] using the RUSLE model, generated the soil erosion hazard map for the Nzoia basin with an average annual soil loss rate of 0.51 and a maximum of 8.84 Mton ha⁻¹ yr⁻¹, which translates to a mean annual soil loss of 657,900 Mton/yr. A study by [29] using the SWAT model in the basin projected a sediment load of 3,767.9 tons per month, or 45,216 tons per year, for the year 2030, compared to a sediment load of 1,400.79 tons per month, or 16,809 tons per year, in 1990. Measurements conducted by [3] at the Nzoia River found that the average Total Suspended Solids (TSS) was approximately 466 mg/L, with an average flow rate of about 170 m³/s, translating to a catchment sediment yield of around 2,504,367 tons per year. These results highlight a significant variation between the modelled and measured data, with the modelled results being considerably underestimated. This discrepancy underscores the need for improvements in the modelling processes.

Soil erosion causes many issues, including land degradation, sedimentation of lakes and ecological degradation. Of particular concern is the impact of soil erosion on Lake Victoria, into which the Nzoia River drains. As eroded soil enters the lake, it brings with it excess nutrients and contaminants. This influx contributes to the process of eutrophication and overall decline in water quality. This environmental degradation has a ripple effect on human activities, impacting various economic sectors that rely on the lake's natural resources and ecosystem services. The analysed satellite images of Lake Victoria show the propagation of sediment plumes in the Winam Gulf towards the main lake [5], and this can be attributed to rampant deforestation and other poor land use practices that accelerated soil erosion in the catchment [6]. In response to national and international pressure, the government of Kenya carried out evictions of people who had encroached into forests at Mt. Elgon, Cherangany, Embobut, and Mau complex to prevent the remaining parts as she tries to re-afforest [7]; [8]; [9]; [10].

Considering the discussed aspects, the Nzoia River Basin in Kenya is a critical ecological and agricultural region threatened by soil erosion and sedimentation, exacerbated by unsustainable land management practices, deforestation, and population pressure. As land degradation intensifies, understanding the spatial erosion and sediment delivery process within the basin becomes essential for several reasons. First, it helps identify areas prone to erosion and sedimentation, enabling targeted conservation efforts. Second, quantifying sediment delivery ratios provides insights into the impact of sediment on water quality and aquatic ecosystems in the Nzoia River and its tributaries. Third, developing a comprehensive sediment delivery model is crucial for implementing sustainable agricultural practices that mitigate the adverse effects of erosion while enhancing productivity. This study aims to (a) assess the basin's erosion susceptibility using the RUSLE model, (b) simulate the spatial sediment delivery process, and (c) conduct scenario analysis to determine the most effective soil erosion control strategies.

MATERIALS AND METHODS

Study area

The Nzoia Basin lies geographically between latitude 0^o 03' N to 1^o 29'N and longitude 34^o 01'E to 35^o 43'E (see Figure 1) and administratively transverses Uasin Gishu, Trans Nzoia, Kakamega and Busia counties of Kenya. It is home to the populous Luyha, Luo and Kalenjii ethnic groups of Western Kenya. The area is generally characterised by moderate to steeply sloping terrain with slopes between 0^o and 46.98^o. Rainfall in this region has an annual average of about 900mm, and the annual amount varies from 2000mm in the highlands to 1000mm in the southwest and lowlands along the lakeshore. Geological studies have shown that the area mainly comprises quaternary and tertiary volcanic deposits, and this area's dominant soil texture is clay loam. Rainfalls exhibit a bimodal pattern with long and short rainy seasons from March to June and August to November, respectively [11].

The region's economy is still primarily rural-based, and more than 90% of the population earns its living

from agriculture and livestock. The farms are mostly privately owned and, on average, sizes of one to three hectares. However, large commercial farms with an average size of 50 to 100 hectares can be found in Trans Nzoia and Uasin Gishu counties. The main food crops grown in the region include maize, sorghum, millet, bananas, groundnuts, beans, potatoes, and cassava, while the cash crops consist of coffee, sugar cane, tea, wheat, rice, sunflower and horticultural crops. A mix of dairy and traditional livestock-keeping farming is also practised in the region [12].

Materials

For this study, the following maps and data were used:

- Rainfall data and coordinates of the stations (source: Kenya Metrological Department).
- Digital Elevation Model (source: <https://csidotinfo.wordpress.com/data/srtm-90m-digital-elevation-database-v4-1/>).
- Soil map (source: <https://data.isric.org/geonetwork/srv/api/records/4648929a-8031-49cc-9d56-9f3aeff2f8d9>).
- Land use map (source: <https://worldcover2021.esa.int/downloader>).

The models applied in this study are:

- Integrated Land and Water Information System (ILWIS), version 3.8.6
- ArcMap 10.1
- Microsoft-Excel

Methodology

A method that integrates Revised Universal Soil Loss Equation (RUSLE), sediment transport, and Geographic Information System (GIS) techniques was formulated and used to assess the susceptibility of the Nzoia River catchment to soil erosion and deposition. The equations relating to factors in the RUSLE and sediment transport capacity (TC) were combined in the ILWIS environment to form potential soil loss and TC functions, which were then applied in subsequent analyses. ILWIS is an acronym for the Integrated Land and Water Information System, and it was developed by the International Institute for Aerospace Survey and Earth Sciences (ITC), Enschede, The Netherlands. It is a Geographic Information System (GIS) with image processing capabilities and provides a platform for efficiently formulating finite equations using the MapCalc functionalities. Calculations in ILWIS can be done on a pixel basis where the effect of the neighbouring pixels is not considered [13]; however, neighbourhood operations is a special spatial analysis in ILWIS that allows calculations on pixels to be dependent on the neighbouring pixels. This capability was utilised to route the detached sediment into the streams and subsequently to Lake Victoria. This enabled the identification of areas in the catchment prone to erosion and deposition as well as in estimation of the average annual sediment load reaching the lake.

The following are the modelling steps (see flow chart in Figure 2):

1. ArcMap 10.1 was applied to delineate, classify, resample, and interpolate relevant maps for the study area. The generated maps included the Digital Elevation Model (DEM), slope, interpolated average monthly and annual rainfall, soil type, and land use.
2. The generated maps were loaded into the ILWIS model.
3. The new function command in ILWIS was used to build RUSLE and TC models.
4. The gross catchment soil loss potential was calculated using the RUSLE model.
5. The single flow sediment routing algorithm was formulated and applied to route the detached sediment into the river channels and Lake Victoria. This process enabled the establishment of erosion and deposition zones over the river catchment.
6. Scenario assessment of soil erosion control practices was undertaken, and their efficiencies were evaluated.

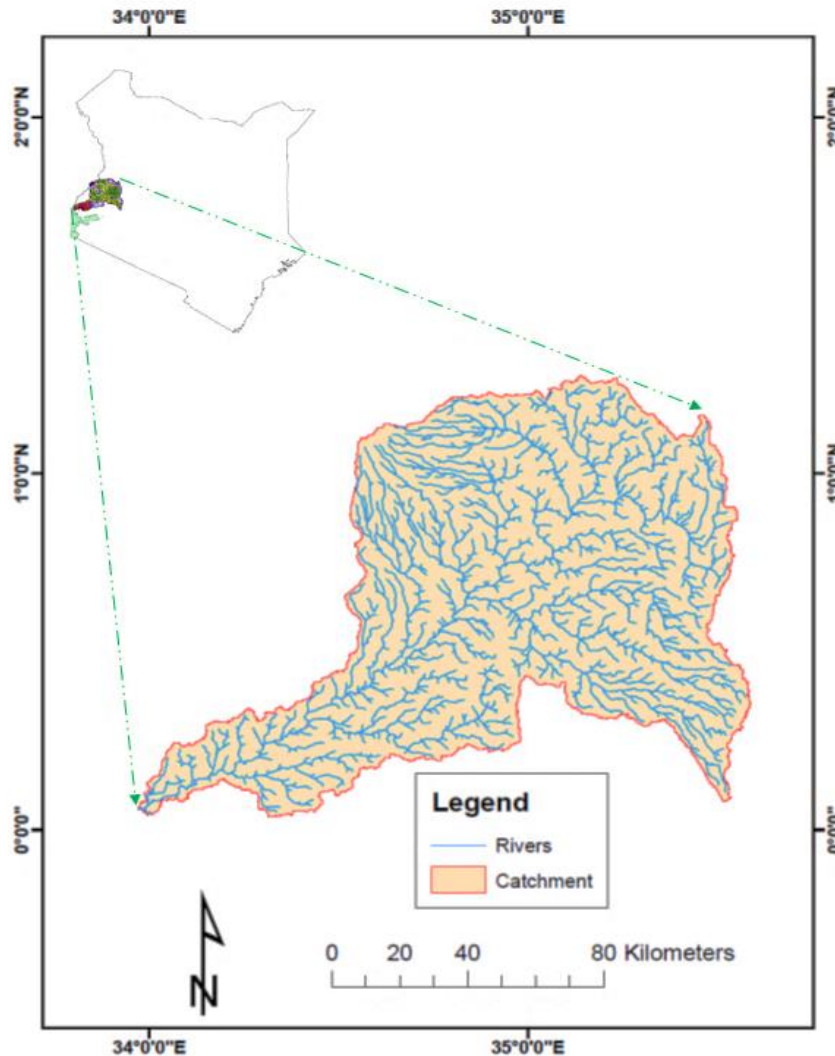


Figure 1: River Nzoia catchment in Kenya

Calculation of RUSLE factors in ILWIS GIS

RUSLE is an empirically based model that can predict the long-term average annual rate of soil erosion on slopes using data on rainfall patterns, soil type, topography, crop system and management practices [14]. It retains the factors of the USLE by including improved means of computing soil erosion factors. The RUSLE model in a GIS environment can predict erosion potential on a cell-by-cell basis, and it was applied in this study to estimate potential annual soil loss. This equation is a function of five input factors: rainfall erosivity, soil erodibility, slope length and steepness, cover management and support practice [14]; [15]; [16]; [17]. These factors vary over space and depend on other input variables [18]. The RUSLE equation is given by equation (1);

$$E = R \times K \times LS \times C \times P \tag{1}$$

Where E is mean annual soil erosion (tons ha^{-1}), R is the rainfall erosivity factor ($MJ\ mm\ ha^{-1}\ h^{-1}$), K is the soil erodibility factor (tons $h\ MJ^{-1}\ mm^{-1}$), LS is the topographic factor (-), C is the crop and management factor (-), and P is the erosion control practice factor (-). In the ILWIS model, raster maps of the RUSLE factors were generated based on the adopted equation relating to the factor or by adopting values found in the existing literature. This was then used to estimate soil loss within each pixel of the resultant map

Calculation of RUSLE factors in ILWIS GIS

The rainfall erosivity factor (R) measures rainfall's effect on erosion. The R factor is a summation of various properties of rainfall, including intensity, duration, and size of water drops. In this study, the estimated

values for the R factor were undertaken using an equation (2) as recommended by various studies [20]; [18]; [27].

$$R = \sum_{i=1}^{12} 1.735 \times 10^{\left(1.5 \log_{10} \left(\frac{P_i^2}{P} \right) - 0.08188 \right)} \quad (2)$$

Where R is the rainfall erosivity index ($\text{MJ mm ha}^{-1} \text{h}^{-1} \text{y}^{-1}$), P_i is the mean rainfall depth in the month (mm), and P (mm) is the mean annual rainfall in a rainfall station. Point rainfall erosivity for each rainfall station was generated using equation (2), whereby the 50 rain gauge stations within and around the study area were considered. The rainfall data for the study area were obtained from the Kenya Meteorological Department (KMD) and were available in cumulative daily rainfall format for the year 1990 to 2012. The data were filled using the inverse distance weighting method and applied to calculate the R factor. The spatial distribution of rainfall erosivity (R) in the study area was estimated using the Kriging interpolation method in ArcMap 10.1, and the values attained show variation between 700 and 5200 $\text{MJ mm ha}^{-1} \text{h}^{-1} \text{year}^{-1}$ (see Figure 3).

Soil erodibility factor (K) measures the resistance of the soil to detachment and transportation by raindrop impact and surface runoff. K factor is a function of the inherent soil properties, including organic matter content, particle size and soil permeability. The Williams equation (3) was used to estimate the K factor as suggested by several studies [19]; [20]; [21]; [22]. The equation is given below:

$$K = 0.1317 \cdot f_{csand} \cdot f_{cl-si} \cdot f_{orgc} \cdot f_{hisand} \quad (3)$$

Where f_{csand} (fraction of coarse sand) decreases the K factor values in soils with high coarse sand and increases for soils with little sand; f_{cl-si} (ratio of the fraction of clay to silt) reduces K factor values for soils containing a high proportion of clay to silt; f_{orgc} (fraction of organic carbon) reduces K values in soils with high organic carbon content, while f_{hisand} (fraction of high sand) reduces K values for soils with excessively high sand concentrations.

$$f_{csand} = \left(0.2 + 0.3 \cdot \exp \left[-0.256 \cdot m_s \cdot \left(1 - \frac{m_{silt}}{100} \right) \right] \right) \quad (4)$$

$$f_{cl-si} = \left(\frac{m_{silt}}{m_c + m_{silt}} \right)^{0.3} \quad (5)$$

$$f_{orgc} = \left(1 - \frac{0.25 \cdot orgC}{orgC + \exp[3.72 - 2.95 \cdot orgC]} \right) \quad (6)$$

$$f_{hisand} = \left(1 - \frac{0.7 \cdot \left(1 - \frac{m_s}{100} \right)}{\left(1 - \frac{m_s}{100} \right) + \exp \left[-5.51 + 22.9 \cdot \left(1 - \frac{m_s}{100} \right) \right]} \right) \quad (7)$$

Where m_s is the per cent sand content (0.05 - 2.00 mm diameter particles), m_{silt} is the per cent silt content (0.002 - 0.05 mm diameter particles), m_c is the per cent clay content (< 0.002 mm diameter particles), and $orgC$ is the per cent organic carbon content of the layer, % [21]; [22].

This study acquired soil data from the Soil and Terrain Database for Kenya (KENSOTER database). The soil information extracted from the database for use in the assessment of soil erodibility included fractions of sand, silt, clay, and organic carbon in the soil. Equation (3) was built in ILWIS and applied to generate a raster map of the K factor. The K -factor varied between 0 and 0.03 tonnes h $\text{MJ}^{-1} \text{mm}^{-1}$ (see Figure 4).

The slope length factor (L) accounts for the effects of slope length on the erosion rate, while the slope steepness factor (S) accounts for the effects of slope angle on erosion rates. The combined LS factor for the catchment was computed using equation (8) as recommended by various studies [18]; [24]; [25].

$$LS = \left(\frac{\text{Flow accumulation} \times \text{Cell size}}{22.13} \right)^{0.4} \times \left(\frac{\sin(s)}{0.0896} \right)^{1.3} \tag{8}$$

Where LS is the combined slope length and slope steepness factor, and s is the slope in degrees. Cell size is the grid cell size (for this study, it is 92.459 m). The value of the LS factor in the study area varies from 0 to over 80 in sloppy regions (see Figure 5).

The crop/vegetation management factor (C) accounts for the influence of cover management practices such as tillage practices, cropping types, crop rotation, and fallow on soil erosion rates (see Figure 6). The support practice factor (P) accounts for the influence of support practices such as contouring, strip cropping, and reverse bench terracing on erosion rates. The values of P and C factors found in [17] and [23] were adopted for this study (see Table 1).

Calculation of Sediment Transport Capacity

In this study, the annual sediment transport capacity was calculated on a pixel basis based on equation (9), as suggested by [15] and [16].

$$TC = ktc \times R \times K \times A^{1.4} S^{1.4} \tag{9}$$

Where TC is the transport capacity ($\text{tons ha}^{-1} \text{ year}^{-1}$), and ktc is the transport capacity coefficient used for calibration. R and K are the rainfall erosivity and the soil erodibility factors of the RUSLE equation, A is the upslope drainage area (m^2), and S is the local slope gradient (m m^{-1}). Equation (9) was modified by replacing area A with a product of the flow accumulation map and the pixel's area, and S by Tangent of slope map (see equation 10);

$$TC = ktc \times R \times K \times (\text{Flow Accumulation} \times \text{Pixel Area})^{1.4} \times (\text{Tan}(\text{Slope}))^{1.4} \tag{10}$$

Table 1: Values of C and P parameters

<i>Support Practice</i>	<i>P Factor</i>	<i>Crop Type</i>	<i>Crop Factor</i>	<i>Tillage Method</i>	<i>Tillage Factor</i>
Contouring: 0 – 1° slope	0.60	Croplands-Maize	0.600	Fall plow	1.00
Contouring: 2 – 5° slope	0.50	Grassed plains	0.050	Spring plow	0.90
Contouring: 6 – 7° slope	0.60	Swamps	0.000	Mulch tillage	0.60
Contouring: 8 – 9° slope	0.70	Forests	0.002	Zone tillage	0.25
Contouring: 10 – 11° slope	0.80	Shrubs	0.010	No-till	0.25
Contouring: 12 – 14° slope	0.90	Woods	0.008	Ridge tillage	0.35
Reverse-slope bench terrace	0.05				
Level bench terrace	0.14				

Note: C – FACTOR = Crop Factor \times Tillage Factor

Source: [17]; [23]

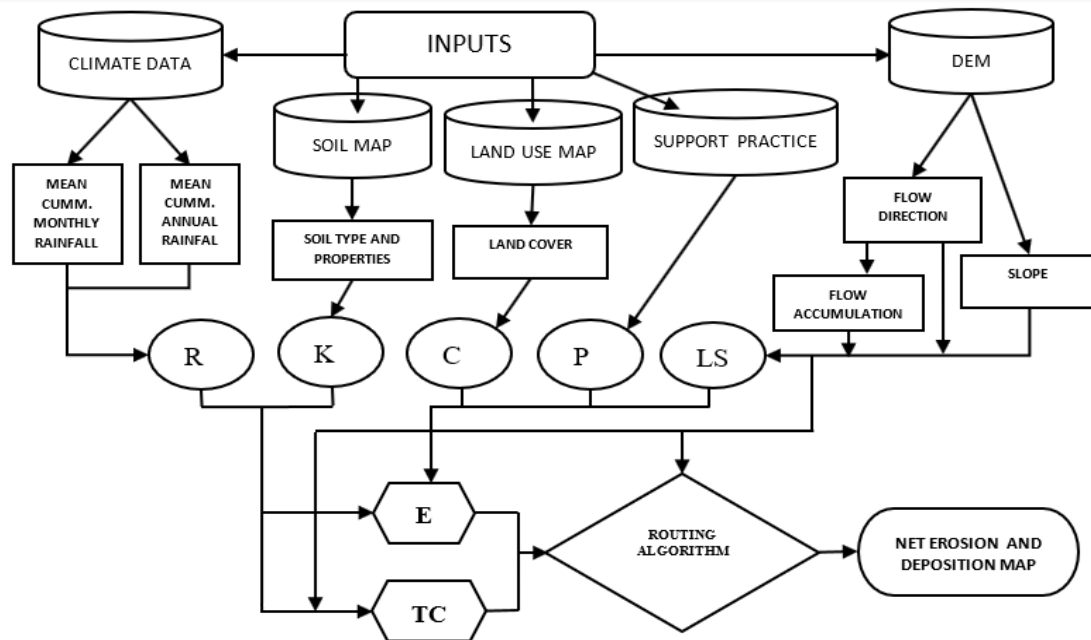


Figure 2: Flow chart of the modelling process

Routing of detached sediments

A single flow algorithm was developed and applied to route the detached sediments towards river channels and finally to the sink (lake). The developed algorithm is applied in the Neighbourhood and iteration functionalities of the ILWIS model, whereby the outcome of pixel calculation depends directly on the values of neighbouring pixels. Neighbourhood calculations use an imaginative matrix window of 3x3 cells that repeats a specified calculation on every pixel in the map, taking into account the values of its neighbours. The calculation window starts with the first pixel on the map's first row, storing the result in the central pixel. Then, the calculation window moves to the second pixel in the first line, repeating the calculation over the entire map. If a neighbourhood operation is performed on a pixel on the top or bottom line or the very first or last column of a raster map, new neighbours are created by duplicating this boundary line or column (<https://ftp.itc.nl/pub/ilwis/pdf/usrch09.pdf>).

In formulating the routing algorithm, the following conditions were taken into consideration:

- Sediments are routed along runoff patterns towards the rivers and the lake.

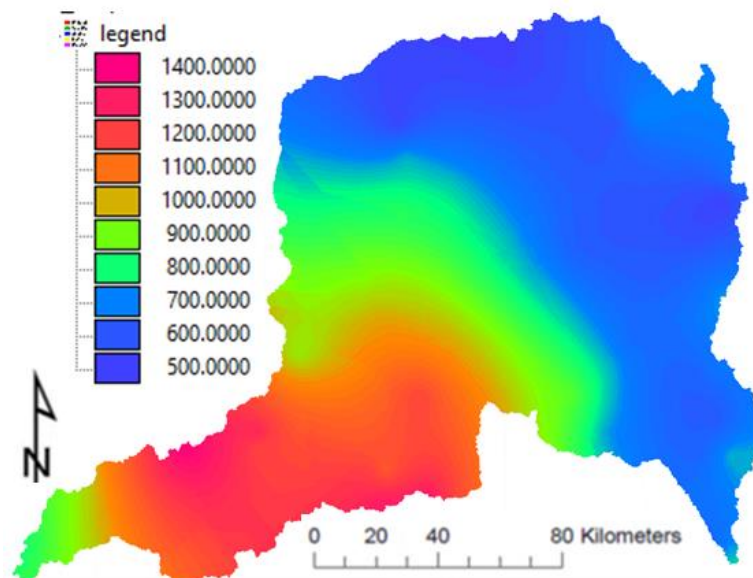


Figure 3: Spatial variation of R factor.

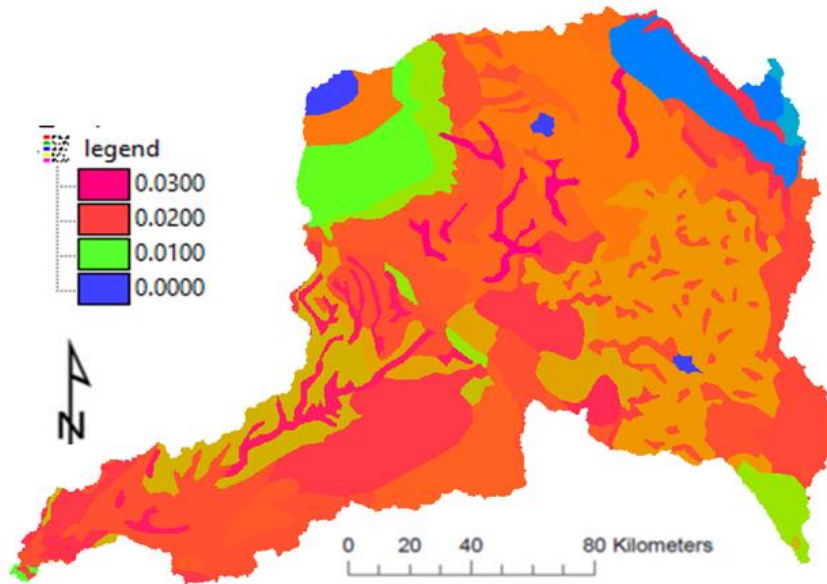


Figure 4: Spatial variability of K factor over the catchment.

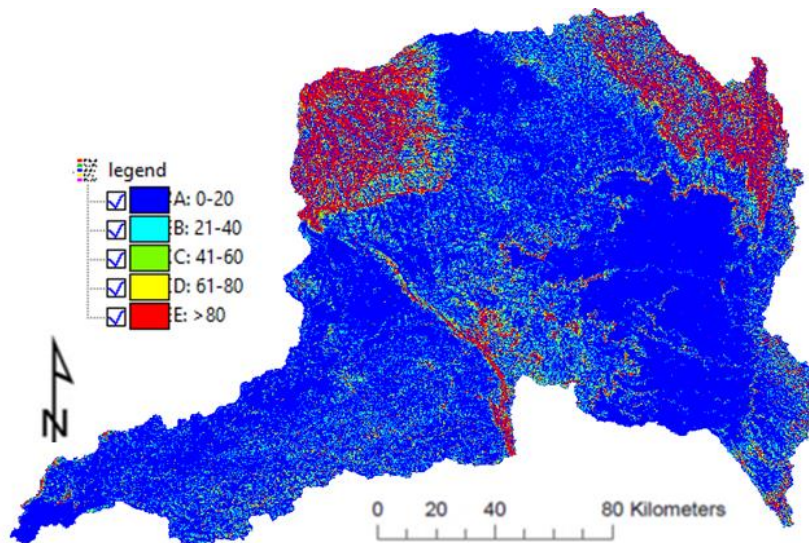


Figure 5: Spatial variability of LS factor over the catchment.

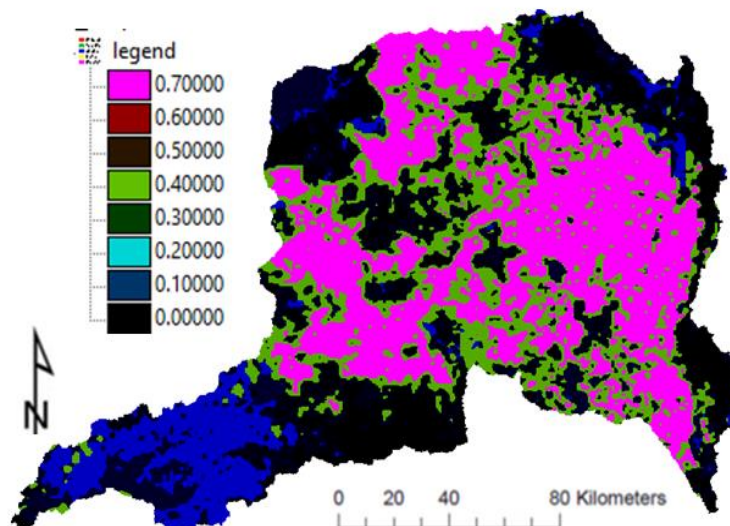


Figure 6: Spatial variation of C factor.

- In the imaginative window of 3x3 cells, the central cell (numbered 5) receives the calculated value at any iteration or calculation step.
- If the central cell's TC is greater or equal to its sediment flux, sediment transport equivalent to the current sediment flux is modelled; otherwise, sediment deposition equivalent to the cell's current flux is modelled.
- If the neighbouring cell's TC is smaller than its sediment flux, then zero sediment transport is modelled; otherwise, sediment transport equivalent to the cell's sediment flux is modelled.
- The sediment transport modelled in the neighbouring cell will be added to the central cell if the neighbouring cell's flow direction is towards the central cell.
- The TC of river channels was assumed to be always greater than the sediment flux.

Calibration procedure

A sediment measurement in a study by [3] established that the average Total Suspended Solids (TSS) in the Nzoia River basin was approximately 466 mg/L with an average flow rate of about 170 m³/s. This corresponds to a catchment sediment yield of about 2,504,367 tons/year, and this case will be simulated to calibrate the formulated model. During the calibration process, the *ktc* coefficient in the sediment transport capacity equation is varied until the modelled sediment yield result agrees with the value reported in the literature.

RESULTS AND DISCUSSIONS

Soil erosion modelling using RUSLE

Figure 7 is the land use map of the Nzoia basin for the year 2021, and the dominant land use in the basin is the agricultural production of cereals mainly maize (cropland), which takes up about 54% of the catchment area. The RUSLE model was applied to generate the potential annual soil loss for the catchment, and the erosion yield results were classified into four categories:

- Low erosion (LE) for erosion yields between 0 and 5 tonnes per hectare per year.
- Moderate erosion (ME) for erosion yields between 5 and 20 metric tonnes per hectare per year.
- High erosion (HE) for erosion yields between 20 and 30 metric tonnes per hectare per year.
- Severe erosion (SE) for erosion yields above 30 tonnes per hectare per year.

In the simulation of the current state of soil erosion, it was assumed that no erosion control practice was being applied at the catchment (RUSLE's P factor = 1). The potential annual soil loss map, shown in Figure 8, indicates that the percentage of the catchment that had low erosion was 69.9%, 18.5% for Moderate erosion, 6.7% for high erosion, and 4.9% had severe erosion. The weighted average annual soil loss for the catchment was 6.7 tonnes/ha/year, or a total catchment soil loss potential of about 8.38×10^6 tonnes/year. This value is significantly higher than the value modelled in [28] and [29]. From the map, the areas around Kapsokwony, Kipkarren, Lessos, and Cherangani are erosion-prone. This may be partly attributed to the nature of the topography, which is primarily sloppy. These regions also have high population densities, and in some cases, people encroach on marginal areas to grow subsistence crops or burn charcoal, thereby increasing the region's susceptibility to erosion.

Sediment routing

According to [17], not all the sediment detached from hillslopes finds its way into the river system, as some is deposited on foot slopes and in floodplains, where it remains in temporary storage, sometimes until the next storm. Reference [26] noticed a general decline in sediment yield with an increase in the catchment area and sediment transport distances, which can be attributed to sediment being deposited in sinks, reducing erosion rates. The transport capacity of surface runoff also influences whether detached soil materials are deposited or transported [17].

In this section, the sediments detached based on the present conditions of the catchment, and assuming that no erosion control management or support practices are in place, are routed downstream based on the

formulated sediment routing algorithm. In the formulation of this algorithm, the direction of the flow of sediments is guided by the flow direction map while taking into account the transport capacity of each pixel. If the pixel's TC is smaller than the modelled erosion, then sediment deposition equivalent to the cell's current sediment flux is modelled; otherwise, sediment yield equivalent to the cell's flux is transported to the receiving neighbouring pixel. To estimate the sedimentation yield in Lake Victoria from the River Nzoia basin, several iterations of the sediment routing algorithm must be undertaken until there are no changes in sediment loss. The process proved tedious when using high-resolution maps. Therefore, the input maps were resampled to a lower resolution of 924.5 m by 924.5 m, which enhanced the simulation. It now takes about 250 spatial steps to complete the process. The plot in Figure 9 summarizes the model calibration process as a function of the *ktc* factor. Using a *ktc* value of 0.000012 results in a cumulative sediment yield of 2,494,575 tons per year at Lake Victoria, which deviates from the value measured in [3] by only 0.39%. This translates to a catchment sediment delivery ratio (SDR) of about 29%. The calculated SDR is twice the value determined in [28], indicating the severity of erosion in the catchment. Figures 10, 11, 12, 13, and 14 illustrate the transfer process of detached sediments by overland flows into river channels, eventually reaching Lake Victoria.

Identification of erosion and deposition sites

To identify sites where erosion or deposition occurred, the map generated from the calibrated single-flow sediment routing algorithm is subtracted from the gross erosion map which was derived from the RUSLE model. From the resultant map, regions with positive values are erosion zones, regions with negative values indicate deposition zones and regions with zero values are zones of neither erosion nor deposition. Figure 15 is the map showing erosion or deposition sites, and it is classified into five categories:

- Low deposition (LD) for deposition of less than 5 tonnes per hectare per year.
- Excessive deposition (ED) for deposition greater than 5 tonnes per hectare per year.
- No deposition nor erosion (no E or D) for zero net erosion or deposition.
- Tolerable erosion (TE) for net erosion less than 20 tonnes per hectare per year.
- Severe erosion (SE) for net erosion above 20 tonnes per hectare per year.

The result obtained shows that approximately 5% of the catchment had ED, 11% had LD, 36% had no E or D, 42% had TE and 6% had SE. These results prove that not all detached soil sediment can be moved from the place of origin. Also, the feet of mountainous regions generally had severe deposition which results from a general reduction in the transport capacity of runoff as the slope decreases, thus depositing sediments from the uplands.

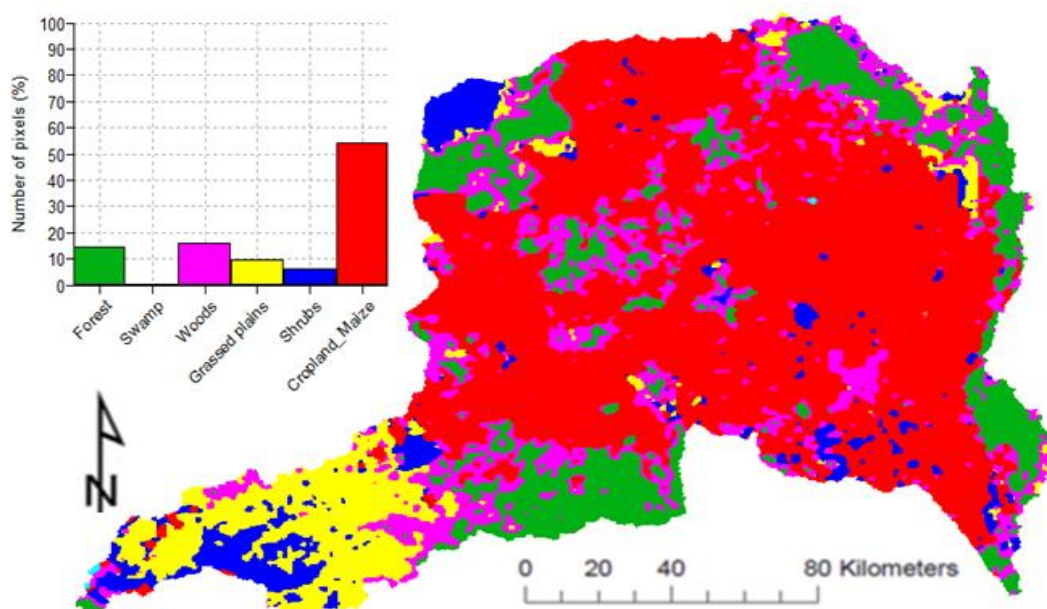


Figure 7: Land use map of Nzoia catchment for the year 2021.

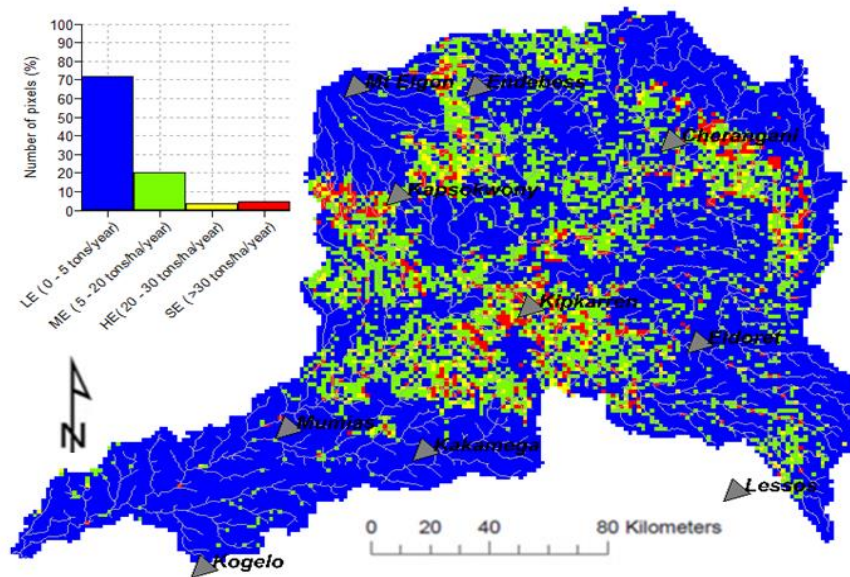


Figure 8: The current state of soil loss potential in the catchment.

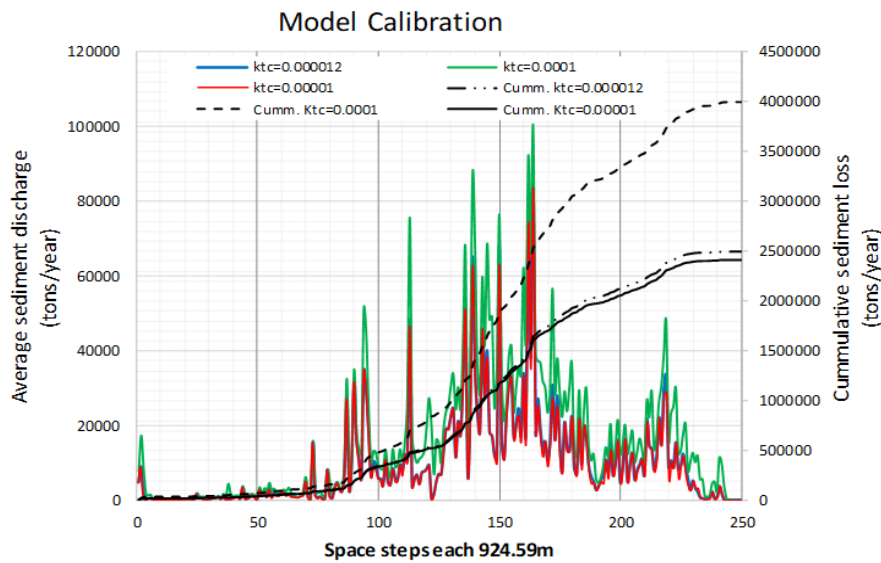


Figure 9: Plot showing the influence of *ktc* factor on lake sedimentation rate

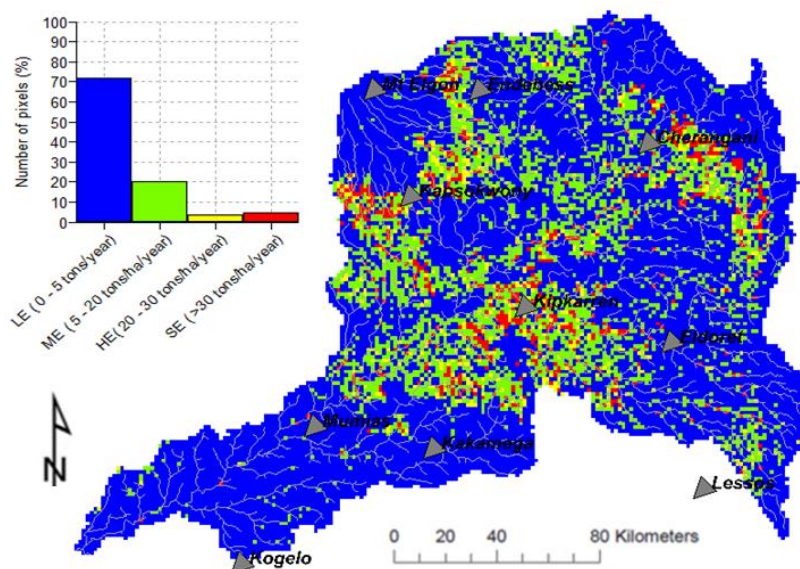


Figure 10: Map showing the potential soil detachment in the catchment before sediment routing.

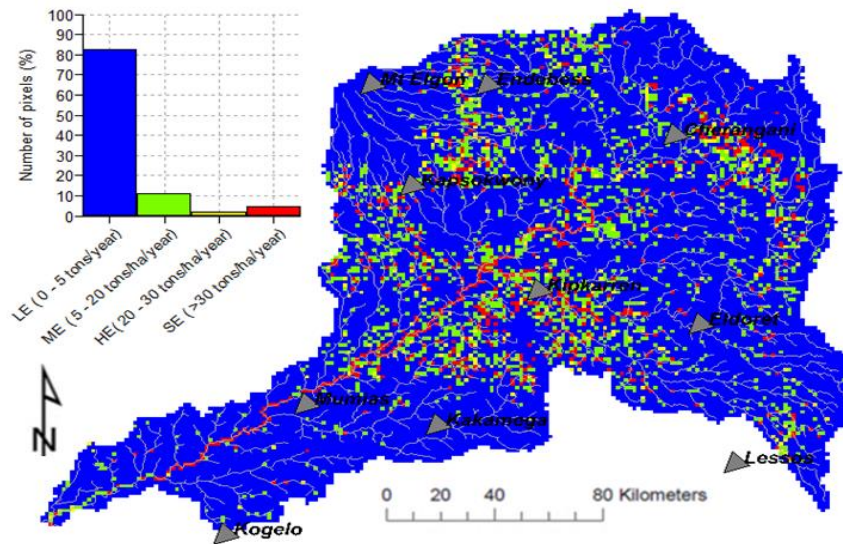


Figure 11: State of sediment transfer into river channels after 50 iterations.

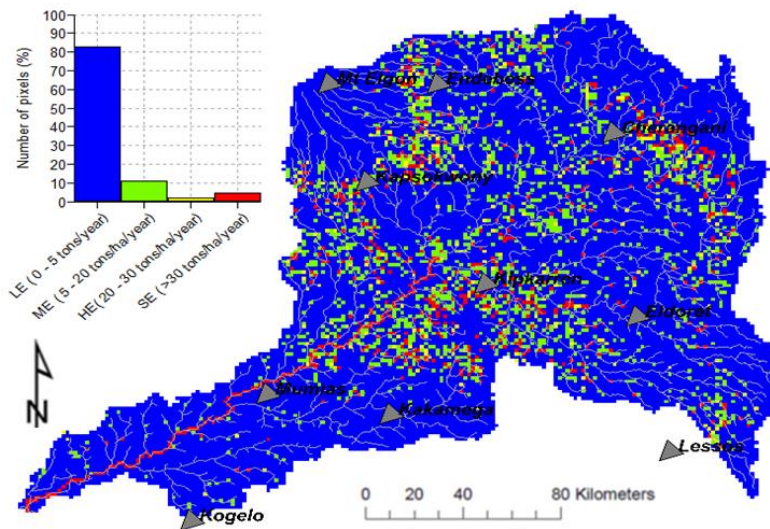


Figure 12: State of sediment transfer into river channels after 100 iterations.

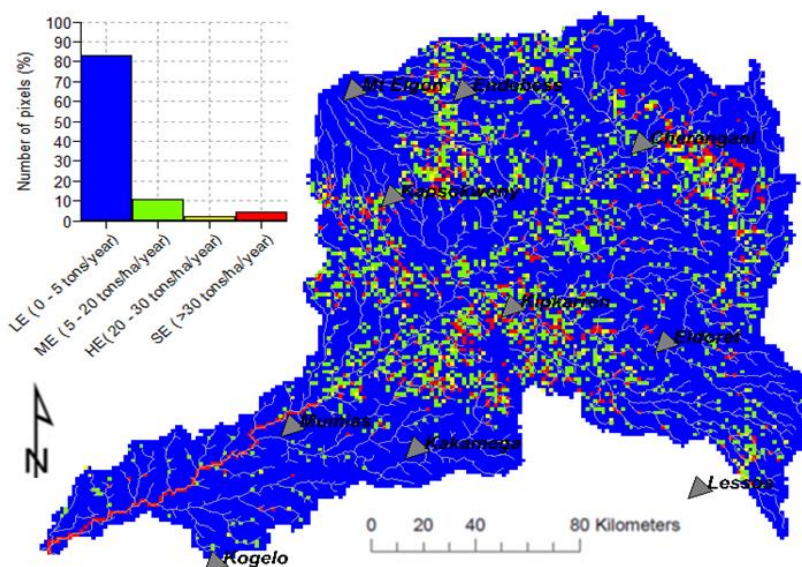


Figure 13: State of sediment transfer into river channels after 150 iterations.

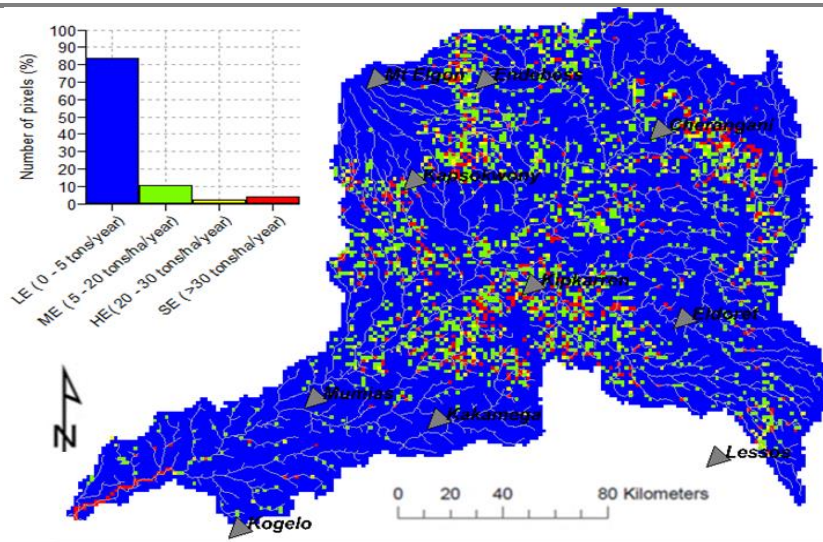


Figure 13: State of sediment transfer into river channels after 200 iterations.

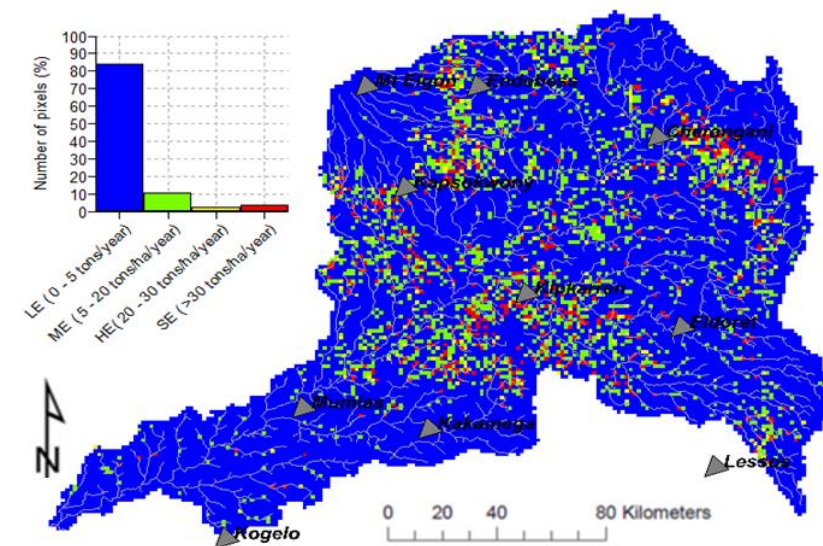


Figure 14: State of sediment transfer into river channels after 250 iterations.

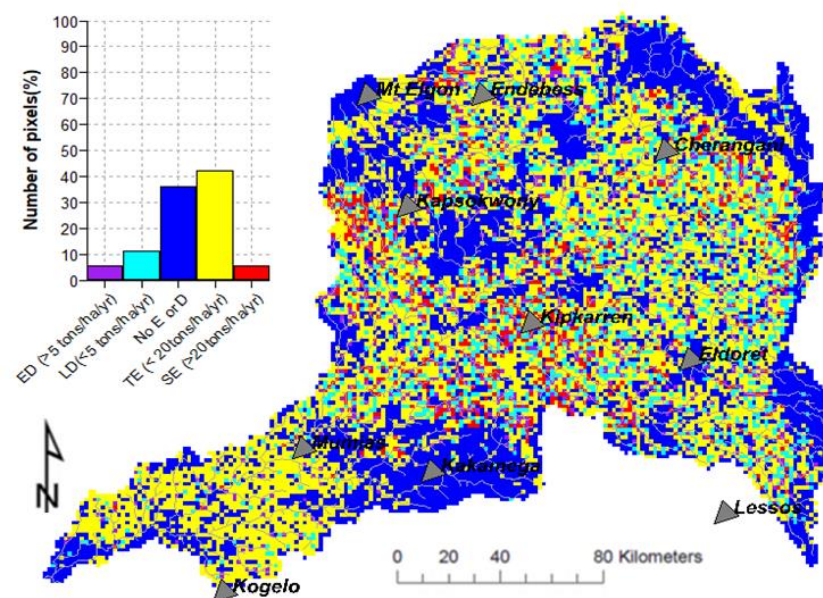


Figure 15: Map showing erosion and deposition sites after sediment routing.

Scenario analysis of erosion control practices

A mean annual soil loss of 11 to 20 tonnes ha⁻¹ is generally considered acceptable [17]. As shown in Figure 8, regions classified as high erosion (HE) and severe erosion (SE) had erosion yields exceeding this tolerable range, accounting for about 12% of the catchment area. A comparison between Figures 7 and 8 revealed that cropland areas were the main contributors to soil erosion in the catchment. Practical agronomic and mechanical soil erosion control methods were applied, either individually or in combination, to the cropland areas. Their effectiveness was assessed and quantified based on their ability to reduce the basin's soil loss potential to an acceptable level. The analysis included various methods, such as 20-meter intervals contours, level bench terraces, and reverse bench terracing for mechanical approaches, as well as afforestation, mulch till, no-till, and fall plow for agronomic practices.

1. Application of a Single Soil Erosion Control Method

This section tested the efficiency of each mechanical and agronomic erosion control method. The following are a brief description of simulations that were undertaken, Table 2 shows the summary of the results obtained and Figure 16 is an efficiency inter-comparison plot.

- *CS_fallplow*: Determination of the current state of soil loss potential using RUSLE model assuming adoption of fall plow tillage condition in croplands and no erosion control practices in agricultural fields (i.e., RUSLE's *P*-factor = 1).
- *Afforest_CL_notill*: Determination of soil loss potential using RUSLE model assuming afforestation of croplands under no-till condition in croplands.
- *Cont20m_CL_fallplow*: Determination of soil loss potential using RUSLE model with assumed adoption of contouring 20m interval under fall plow tillage condition in croplands.
- *LBT_CL_fallplow*: Determination of soil loss potential using RUSLE model with assumed adoption of level bench terraces under fall plow tillage conditions in croplands.
- *RBT_CL_fallplow*: Determination of soil loss potential using RUSLE model with assumed adoption of reverse bench terraces under fall plow tillage conditions in croplands.
- *Cont20m_CL_fallplow*: Determination of soil loss potential using RUSLE model with assumed adoption of contouring 20m interval under fall plow tillage condition in croplands.
- *Cont20m_CL_mulchtill*: Determination of soil loss potential using RUSLE model with assumed adoption of contouring 20m interval under mulch tillage condition in croplands.
- *Cont20m_CL_notill*: Determination of soil loss potential using RUSLE model with assumed adoption of contouring 20m interval under no-tillage condition in croplands.

From Table 2, afforestation of croplands registered high efficiency, with 99.93% of the basin area under allowable erosion (i.e., erosion yield less than 20 tons/ha/year), and 0.06% under excessive erosion (i.e., erosion yield greater than 20 tons/ha/year). Adoption of this method reduced potential soil loss by 96.5%. This was followed by reverse bench terracing, level bench terracing and contouring at a 20-metre interval in that order. Also, the influence of the tillage method was assessed, and it was established that no-tillage practice conserves soils to a higher degree. The results for assumed afforestation of agricultural fields illustrate the importance of forests in soil erosion control and justify the current government drive to increase forest cover in the country. Even though afforestation proves effective in controlling erosion at the basin, this method is hard to implement since the resident will have to forfeit their lands. This calls for integration of this method with other methods to allow people to practice agricultural activities while afforesting some percentage of their land, especially the sloppy regions and along the river channels.

2. Application of Composite Soil Erosion Control Methods

Applying a single erosion control method can be impracticable due to its repercussions or cost. Afforestation proved to be the best solution for controlling the soil erosion menace, even though its adoption will generally force residents out of their lands which they depend on to earn their living. Therefore, the integration of afforestation with other mechanical methods such as level bench terracing, reverse bench terracing and

contouring with a 20-metre interval was applied in scenario assessment and their efficiencies were assessed. The following are brief description of simulations that were undertaken, and Table 2 shows the summary of the results attained:

- *RBT_115deg_afforest_ge15deg_FP*: Determination of basin's soil loss potential using RUSLE model with assumed adoption of reverse bench terracing in cropland with slope less than 15 degrees and afforestation of cropland with slope greater than 15 degrees under fall plow tillage conditions.
- *LBT_115deg_afforest_ge15deg_FP*: Determination of basin's soil loss potential using RUSLE model with assumed adoption of level bench terraces in cropland with slope less than 15 degrees and afforestation of cropland with slope greater than 15 degrees under fall plow tillage conditions.
- *Cont20m_115deg_afforest_ge15deg_FP*: Determination of basin's soil loss potential using RUSLE model with assumed adoption of contouring with a 20-metre interval in cropland with slope less than 15 degrees and afforestation of cropland with slope greater than 15 degrees under fall plow tillage conditions.
- *Cont20m_15deg_LBT_115deg_afforest_ge15deg_FP*: Determination of basin's soil loss potential using RUSLE model with assumed adoption of contouring at a 20-metre interval in cropland with slope less than 5 degrees, Level bench terraces in cropland with slope between 5 and 10 degrees, and afforestation of cropland with slope greater than 15 degrees under fall plow tillage conditions.
- *Cont20m_15deg_LBT_115deg_afforest_ge15deg_MT*: Determination of basin's soil loss potential using RUSLE model with assumed adoption of contouring at a 20-metre interval applied to slopes less than 5 degrees, level bench terraces in cropland with slope between 5 and 10 degrees, and afforestation of cropland with slope greater than 15 degrees under mulch tillage.
- *Cont20m_15deg_LBT_115deg_afforest_ge15deg_NT*: Determination of basin's soil loss potential using RUSLE model with assumed adoption of contouring at a 20-metre interval applied to slopes less than 5 degrees, level bench terraces in cropland with slope between 5 and 10 degrees, and afforestation of cropland with slope greater than 15 degrees under no-till condition.
- *Cont20m_15deg_RBT_115deg_afforest_ge15deg_FP*: Determination of basin's soil loss potential using RUSLE model with assumed adoption of contouring at a 20-metre interval is applied to slopes less than 5 degrees, reverse bench terraces in cropland with slope between 5 and 10 degrees, and afforestation of cropland with slope greater than 15 degrees under a fall plow tillage condition.
- *Cont20m_15deg_RBT_115deg_afforest_ge15deg_MT*: Determination of basin's soil loss potential using RUSLE model with assumed adoption of contouring at a 20-metre interval is applied to slopes less than 5 degrees, reverse bench terraces in cropland with slope between 5 and 10 degrees, and afforestation of cropland with slope greater than 15 degrees under mulch tillage conditions.
- *Cont20m_15deg_RBT_115deg_afforest_ge15deg_NT*: Determination of basin's soil loss potential using RUSLE model with assumed adoption of contouring at a 20-metre interval applied to slopes less than 5 degrees, reverse bench terraces in cropland with slope between 5 and 10 degrees, and afforestation of cropland with slope greater than 15 degrees under no-till conditions.
- *LBT_15deg_RBT_115deg_afforest_ge15deg_FP*: Determination of basin's soil loss potential using RUSLE model with assumed adoption of level bench terraces for slopes less than 5 degrees, reverse bench terraces in cropland with slope between 5 and 10 degrees, and afforestation of cropland with slope greater than 15 degrees under fall plough tillage conditions.
- *LBT_15deg_RBT_115deg_afforest_ge15deg_MT*: Determination of basin's soil loss potential using RUSLE model with assumed adoption of level bench terraces for slopes less than 5 degrees, reverse bench terraces in cropland with slope between 5 and 10 degrees and afforestation of cropland with slope greater than 15 degrees under mulch tillage condition.
- *LBT_15deg_RBT_115deg_afforest_ge15deg_NT*: Determination of basin's soil loss potential using RUSLE model with assumed adoption of level bench terraces for slopes less than 5 degrees, reverse bench terraces in cropland with slope between 5 and 10 degrees and afforestation of cropland with slope greater than 15 degrees under no-till condition.

In the application of two erosion control methods, afforestation was assigned to a region with a slope greater than 15° (about 1.8% of the agricultural field), while mechanical methods were assigned to other areas. In the

application of three erosion control methods, forest plantations were assigned to regions with slope inclination greater than 15° while one of the mechanical methods was assigned to areas with slope inclination between 0 and 5° (about 78.1% of the agricultural field), and the other mechanical method assigned to regions with slope inclination of between 5° and 15° (about 20.1% of the agricultural field). In the simulation process, the tillage practices were kept constant or varied to assess their influence in the combination.

The results in Table 2 indicate a general increase in efficiency as more erosion control methods are used, and some combinations perform in the range equivalent to the single application of the afforestation method to cropland. The best combination of the two methods is adopting reverse bench terracing under no-till conditions to regions in agricultural fields with slope inclination less than 15° and afforesting regions with slope inclination greater than 15°. This combination reduced potential soil loss by 92%. The best combination of three methods was attained under no-tillage practice when 20m spaced contours were applied for regions with slope inclination between 0 and 5°, reverse bench terracing for areas with slope inclination between 5° and 15° and afforestation of the other regions. This combination reduced potential soil loss by over 95% (see Figure 16).

Table 2: Summary of simulation results

Soil erosion control methods	Potential Erosion yield (tons)	The ratio of yield to that of the current state of erosion (%)	Potential soil loss reduction (%)	Basin area with allowable erosion (<20tons/ha/yr) (%)	Basin area with Excessive erosion (>20tons/ha/yr) (%)
CS_fallplow	8378362.6	100.0	0.0	88.40	11.60
Afforest_CL_notill	292448.0	3.5	96.5	99.93	0.06
LBT_CL_fallplow	2337823.4	27.9	72.1	99.00	1.00
RBT_CL_fallplow	697519.1	8.3	91.7	99.90	0.14
Cont20m_CL_fallplow	5221239.2	62.3	37.7	95.80	4.20
Cont20m_CL_mulchtil	3246790.3	38.8	61.2	97.80	2.20
Cont20m_CL_notill	1519147.5	18.1	81.9	99.40	0.60
RVT_115deg_afforest_ge15deg_FP	673726.3	8.0	92.0	99.80	0.20
LBT_115deg_afforest_ge15deg_FP	1369529.2	16.3	83.7	99.60	0.40
Cont20m_115deg_afforest_ge15deg_FP	4706392.5	56.2	43.8	96.30	3.70
Cont20m_15deg_LBT_115deg_afforest_ge15deg_FP	1369529.2	16.3	83.7	99.62	1.38
Cont20m_15deg_LBT_115deg_afforest_ge15deg_MT	936585.2	11.2	88.8	99.78	2.22
Cont20m_15deg_LBT_115deg_afforest_ge15deg_NT	557759.2	6.7	93.3	99.89	0.11
Cont20m_15deg_RBT_115deg_afforest_ge15deg_FP	673726.3	8.0	92.0	99.86	0.14
Cont20m_15deg_RBT_115deg_afforest_ge15deg_MT	519103.4	6.2	93.8	99.90	0.10
Cont20m_15deg_RBT_115deg_afforest_ge15deg_NT	383808.4	4.6	95.4	99.93	0.08
LBT_15deg_RBT_115deg_afforest_ge15deg_FP	1170556.5	14.0	86.0	99.67	0.32
LBT_15deg_RBT_115deg_afforest_ge15deg_MT	817201.5	9.8	90.2	99.81	0.19
LBT_15deg_RBT_115deg_afforest_ge15deg_NT	508016.0	6.1	93.9	99.90	0.10

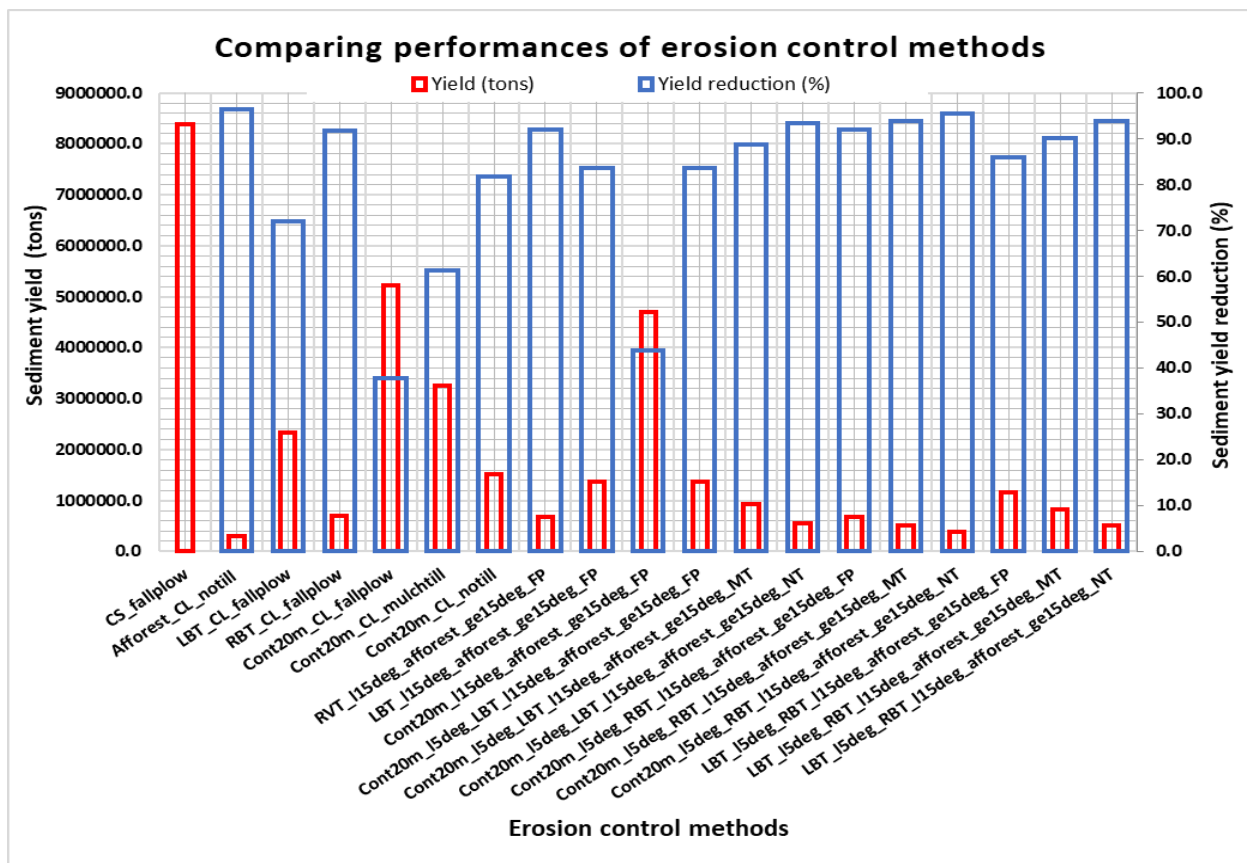


Figure 16: Efficiency inter-comparison plot

CONCLUSION

The erosion risk exists on cultivated land when trees, bushes and grasses are removed. Erosion is accelerated by farming on steep slopes, non-conservation tillage methods, single cropping without fallow or rotation, and encroachment of marginal areas [17]. The formulated RUSLE model in ILWIS GIS highlighted the severity of erosion in the Nzoia basin and pinpointed erosion-prone areas as the foothills of Mt. Elgon, Kipkarren, Kapsokwony, and Cherangani. The estimated catchment’s soil loss potential was 8,380,000 tonnes/year and it varied over the catchment, ranging from 0 in the lowlands to 4,577 tonnes ha⁻¹ per year in sloping areas around Mt. Elgon, Cherangani, and Kipkarren. These results indicate that some regions in the catchment eroded at rates higher than the recommended soil loss tolerance of 11–20 tonnes ha⁻¹ per year thus necessitating the adoption of soil conservation practices.

Implementing soil conservation practices provides full economic use of land while limiting its deterioration. The cropland regions were the dominant contributors of eroded sediments in the basin and a scenario assessment of various soil erosion control methods applied specifically to these regions was undertaken. The simulation results established that adopting more than one erosion control practice will significantly reduce soil erosion, especially if afforestation is restricted to sloping areas while other methods that allow enhanced farming are assigned to relatively flat regions. Forest plantations under no-till conditions applied over the entire cropland reduced catchment’s potential soil loss by about 97% and proved to be efficient when individually applied, though it is impractical to adopt as it will lead to the massive displacement of people who solely depend on farming to earn a living. The results for integrating two soil conservation methods showed that adopting afforestation in cropland regions with slope inclination greater than 15° and reverse bench terracing in other areas of croplands proved effective, with results showing a reduction of the catchment’s potential soil loss by about 92%. Whereas, for integration of three erosion control practices shows that the application of 20m spaced contours in cropland regions with slope inclination between 0 and 5°, reverse bench terracing in cropland regions with slope inclination between 5° and 15° and adopting afforestation method in cropland regions with slope greater than 15° had over 95% reduction of catchment’s soil loss potential. This proves the effectiveness of adopting numerous erosion control methods. Also from

scenario analysis, no-till and mulch tillage proved to be effective in conserving soil and should always be encouraged in farming.

In routing the detached sediments, the basin's sediment yield at Lake Victoria was found to be 2,494,575 tons per year, translating to a catchment sediment delivery ratio of about 29%. This highlights the severity of soil erosion in the catchment, as nearly one-third of the total soil eroded from the basin reaches Lake Victoria. The study also revealed that not all detached soil sediment is transported from its point of detachment. Sediment deposition typically occurs at the base of mountainous regions, due to the reduction in runoff transport capacity as the slope decreases.

The greatest limitation of this study was the use of low-resolution maps in sediment routing, which introduced errors in the simulated results. The adoption of low-resolution maps was necessary due to the inability of the iteration function in the ILWIS model to automatically update the input files for the next iteration step. Manually updating the input files during the calculations proved to be a tedious process, making low-resolution maps a more practical choice.

RECOMMENDATION

The spatial erosion and deposition hazard maps generated in this study should be utilized by the Ministries of Environment and Agriculture as effective tools for combating land degradation in the Nzoia River catchment. Additionally, a more accurate study should be conducted using high-resolution maps and the iteration function in ILWIS GIS. This will require modifications to the ILWIS code to enable the model to automatically update certain input files based on the output from the previous iteration step.

REFERENCES

1. Kenya National Bureau of Statistics. 2019 Kenya Population and Housing Census: Volume I: Population by County and Sub-County. November 2019. <https://housingfinanceafrica.org/app/uploads/VOLUME-I-KPHC-2019.pdf> (Accessed 15 July 2024).
2. Mulinge, W., Gicheru, P., Murithi, F., Maingi, P., Kihui, E., Kirui, O. K., & Mirzabaev, A. "Economics of Land Degradation and Improvement in Kenya." *Economics of Land Degradation and Improvement: A Global Assessment for Sustainable Development*, Springer, 2016, pp. 471-498.
3. Okungu, J., and Opango, P. *Pollution Loads into Lake Victoria from the Kenyan Catchment*. Lake Victoria Environmental Management Project, Jinja, Uganda, 2005. ISBN 9987-8976-5-7. <https://aquadocs.org/bitstream/handle/1834/6914/ktf0050.pdf> (Accessed 15 July 2024).
4. Awiti, A. "Improved Land Management in the Lake Victoria Basin: Final Report on the TransVic Project." *World Agroforestry Centre*, vol. 7, 2006, pp. 1–98.
5. Njuguna H., Romero J. R., Khisa P., Ewing T., Antenucci J., Jorg I. & Okungu J. "The Effect of Turbid Inflows into Winam Gulf, Lake Victoria: A 3D Modelling Study with ELCOM-CAEDYM." *The 11th World Lakes Conference*, 31 October–4 November 2006, Nairobi, Kenya, vol. 2, pp. 90-99.
6. Sive, D. "Nzoia on the Noose: Counting the Cost of River Nzoia Basin Degradation." 2 Nov. 2023, <http://repository.eac.int/bitstream/handle/11671/786/Pollution%20loads%20into%20Lake%20Victoria%20from%20the%20Kenyan%20catchment.pdf?sequence=1> (Accessed 15 July 2024).
7. Amnesty International Kenya. *Nowhere to Go: Forced Evictions in Mau Forest*. 30 May 2007. <https://www.amnesty.org/en/documents/afr32/006/2007/en/> (Accessed 15 July 2024).
8. Daily Nation. "KFS Reclaims 2,000 Acres from Moi." 3 June 2012. <https://nation.africa/kenya/news/KFS-reclaim-2000-acres-from-Moi/1056-1419628-1517hffz/index.html> (Accessed 15 June 2024).
9. Daily Nation. "30 Houses Burnt in Forest Eviction." 24 Feb. 2014. <https://nation.africa/kenya/counties/30-houses-burnt-in-forest-eviction--/1107872-2220556-mes2i5z/index.html> (Accessed 15 June 2024).
10. The Standard. "Mau Forest Settlers Demand Compensation." 2010. <https://www.standardmedia.co.ke/rift-valley/article/2000093307> (Accessed 15 June 2024).

11. Lake Basin Development Authority (LBDA). Project Proposal for Feasibility Study: The Nandi Forest Multipurpose Dam Project. 2008. http://www.lbda.co.ke/downloads/HEP_projects/HEP%20Nandi.pdf (Accessed 19 May 2024).
12. Simiyu G. E., Adams D. D., & Esipila T. "Integrated Assessment of Land Use Changes, Organic Carbon, Greenhouse Gases and Spring Water Variability in the Middle Nzoia River Catchment, Kenya." African Global Change Research Grants, 2008. Final Project Report.
13. Van Westen, C. J., and Terlien, M. T. J. "Deterministic Landslide Hazard Analysis in GIS: A Case Study from Manizales, Colombia." *Earth Surface Processes and Landforms*, vol. 21, 1996, pp. 853-868.
14. Prasannakumar V., Shiny R., Geetha N. & Vijith H. "Estimation of Soil Erosion Risk within a Small Mountainous Sub-Watershed in Kerala, India, Using Revised Universal Soil Loss Equation (RUSLE) and Geo-Information Technology." *Geoscience Frontiers*, vol. 3, no. 2, 2012.
15. De Vente J., Poesen J., Govers G. & Boix-Fayos C. "The Implications of Data Selection for Regional Erosion and Sediment Yield Modelling." *Earth Surface Processes and Landforms*, vol. 34, 2009, pp. 1994–2007.
16. Verstraeten G., Prosser I.P. & Fogarty P. "Predicting the Spatial Patterns of Hillslope Sediment Delivery to River Channels in the Murrumbidgee Catchment, Australia." *Journal of Hydrology*, vol. 334, no. 3-4, 2007, pp. 440–454.
17. Morgan, R. P. C. *Soil Erosion and Conservation*. Blackwell Publishing, Malden, USA, 2005.
18. Kumar K. M., Annadurai R. & Ravichandran P.T. "Assessment of Soil Erosion Susceptibility in Kothagiri Taluk Using Revised Universal Soil Loss Equation (RUSLE) and Geo-Spatial Technology." *International Journal of Scientific and Research Publications*, vol. 4, no. 10, 2014.
19. Arnold J.G., Kiniry J.R., Srinivasan R., Williams J.R., Haney E.B. & Neitsch, S.L. "Chapter 22: SWAT Input Data." 2012. http://swat.tamu.edu/media/69365/ch22_input_sol.pdf (Accessed 15 July 2024).
20. Kogo B. K., Lalit K. & Koech R. "Impact of Land Use/Cover Changes on Soil Erosion in Western Kenya." *Sustainability*, vol. 12, no. 9740, 2020. doi:10.3390/su12229740.
21. Radziuk, H., and Świtoniak, M. "Soil Erodibility Factor (K) in Soils under Varying Stages of Truncation." *Soil Science Annual*, vol. 72, no. 1, 2021, <https://doi.org/10.37501/soilsa/134621>.
22. Ejaz N., Elhag M., Bahrawi J., Zhang L., Gabriel H.F. & Rahman K.U. "Soil Erosion Modelling and Accumulation Using RUSLE and Remote Sensing Techniques: Case Study Wadi Baysh, Kingdom of Saudi Arabia." *Sustainability*, vol. 15, no. 3218, 2023. <https://doi.org/10.3390/su15043218>.
23. McKague, K. "Universal Soil Loss Equation (USLE)." March 2023. <https://www.ontario.ca/page/universal-soil-loss-equation> (Accessed 10 July 2024).
24. Habtamu, A. F. "Assessment of Soil Erosion by RUSLE Model Using Remote Sensing and GIS Techniques: A Case Study of Huluka Watershed, Central Ethiopia." M.Sc. thesis, Addis Ababa University, 2018.
25. Sidi Almouctar M.A., Wu Y., Zhao F. & Dossou J.F. "Soil Erosion Assessment Using the RUSLE Model and Geospatial Techniques (Remote Sensing and GIS) in South-Central Niger (Maradi Region)." *Water*, vol. 13, no. 3511, 2021. <https://doi.org/10.3390/w13243511>.
26. De Vente J., Poesen J., Govers G., Boix-Fayos C. & Mahmood A. "The Sediment Delivery Problem Revisited." *Progress in Physical Geography*, vol. 31, no. 155, 2007.
27. Ganasri, B. P., and Ramesh, H. "Assessment of Soil Erosion by RUSLE Model Using Remote Sensing and GIS: A Case Study of Nethravathi Basin." *Geoscience Frontiers*, 2015. <http://dx.doi.org/10.1016/j.gsf.2015.10.007>.
28. Moses, A. N. "GIS-RUSLE Interphase Modelling of Soil Erosion Hazard and Estimation of Sediment Yield for River Nzoia Basin in Kenya." *Journal of Remote Sensing & GIS*, vol. 6, no. 3, 2017, pp. 1–13.
29. Maloba Joseck Joab, Alex Khaemba, Njenga Mburu and Akali Ngaywa Moses. "Effects of Increased Land Use Changes on Runoff and Sediment Yield in the Upper River Nzoia Catchment." *International Journal of Civil Engineering and Technology*, vol. 7, no. 2, 2016, pp. 76–94.